Variational state based on the Bethe-ansatz solution and a correlated singlet liquid state in the one-dimensional t-J model

Kenji Kobayashi
Department of Natural Science, Chiba Institute of Technology, 2-1-1, Shibazono, Narashino-shi, Chiba 275, Japan

Chikaomi Ohe and Kaoru Iguchi
Department of Chemistry, School of Science and Engineering, Waseda University, Tokyo 169, Japan
(Received 10 July 1996)

The one-dimensional t-J model is investigated by the variational Monte Carlo method. A variational wave function based on the Bethe-ansatz solution is proposed, where the spin-charge separation is realized and a long-range correlation factor of Jastrow-type is included. In most regions of the phase diagram, this wave function provides an excellent description of the ground-state properties characterized as a Tomonaga-Luttinger liquid; both the amplitude and exponent of correlation functions are correctly reproduced. For the spin-gap phase, another trial state of correlated singlet pairs with a Jastrow factor is introduced. This wave function shows generalized Luther-Emery-liquid behavior, exhibiting enhanced superconducting correlations and exponential decay of the spin correlation function. Using these two variational wave functions, the whole phase diagram is determined. In addition, relations between the correlation exponent and variational parameters in the trial functions are derived. [S0163-1829(96)05142-9]

I. INTRODUCTION

The anomalous properties found in high-T_c superconducting copper oxides[1] have led to a renewal of interest in strongly correlated electron systems in low dimensions. Among various candidates, the t-J model has attracted considerable attention as a model to describe the cuprate superconductors.[2,3]

For the one-dimensional (1D) t-J model, much progress has been achieved using analytical and numerical techniques.[4] It has been found[5–7] that three main regions can be distinguished in the phase diagram defined by the electron density and the ratio of spin exchange interaction to hopping amplitude, J/t. First, a Tomonaga-Luttinger liquid[8,9] (TLL) holds for small J/t, which is characterized by power-law decay of correlation functions. It has been clarified that the separation of spin and charge degrees of freedom plays an essential role in this region.[10] Second, phase separation takes place for large J/t, where the system is separated into electron-rich and hole-rich phases. Third, there is a region with a gap in the spin excitation spectrum for $J/t>2$ and at small electron densities.

On the other hand, in the 2D t-J model, although some aspects have been obtained so far,[11] many problems are left unresolved. Particularly, the crucial question is whether the features realized in a 1D system, like the charge-spin separation and/or TLL, take place also in a 2D system or not.[12] To obtain a unified and consistent understanding of the 2D t-J model, further research is needed.

The variational Monte Carlo (VMC) method is one of the most powerful and transparent approaches to investigate strongly correlated electron systems.[13] It provides a deeper insight because of its explicit form of the wave function. It is very important to construct a better trial function in the framework of the VMC technique. One way to obtain further insight into the wave function in the 2D t-J model is to extend the wave function realized in a 1D system. For this purpose, examining trial wave functions for 1D systems in detail gives us useful references in the pursuit of the 2D t-J model. We shall study variational wave functions in the 1D t-J model, keeping the possibility of extending to the 2D system in mind.

So far, various kinds of variational functions have been proposed for strongly correlated electron systems.[14–19] The Gutzwiller wave function[20] has been extensively studied for its simplicity, and shown to be a good trial function for the supersymmetric ($J/t=2$) 1D t-J model.[17] This wave function was improved for other values of J/t by introducing a conventional Jastrow-correlation factor, but the expected TLL behavior was not recovered.[17,19] Recently, Hellberg and Mele have introduced a simple trial wave function of Jastrow type.[18] It takes into account the effect of long-range correlations, and shows successfully the anomalous power-law behavior in correlation functions. This wave function has been extended to the 2D t-J model to discuss the TLL instability.[21] However, the properties of the exact ground state are not wholly reproduced by this wave function, especially in the small J/t region.[19]

In this paper we introduce another type of variational wave function. Two kinds of trial functions are introduced. First, we consider a variational wave function based on the Bethe-ansatz solution. In the limit of $J/t\rightarrow 0$, the charge and spin degrees of freedom are completely separated, and the ground-state wave function obtained from the Bethe-ansatz can be written as a product of the two contributions.[10] For finite values of J/t, although the charge and spin are separated, they interact strongly. To take into account this effect, we introduce a Jastrow-type correlation factor into the Bethe ansatz solution for $J/t\rightarrow 0$. It is shown that this wave function has the advantage of providing an excellent description

of the ground-state properties in most regions of the phase diagram; both the magnitude and exponent of correlation functions are correctly reproduced, and a quantitative discussion can be made.

Next, we consider a trial function for small electron densities. For the spin-gap phase, Chen and Lee have proposed a variational function of a gas of noninteracting bound singlet pairs.[6] This wave function corresponds to a Luther-Emery state[22,8] with an infinite correlation exponent. More accurate trial function can be generated by correlating the singlet pairs with a Jastrow factor. This is just our trial wave function for the spin-gap phase introduced in this paper. This wave function shows a generalized Luther-Emery liquid behavior, exhibiting enhanced superconducting correlations and exponential decay of the spin correlation function.

Comparing the energies of the trial function based on the Bethe-ansatz solution and the generalized Luther-Emery state, the entire phase diagram is determined. Evaluating the correlation exponents by a finite-size scaling analysis, the relations between the correlation exponent and variational parameters in these trial functions are derived.

This paper is organized as follows. In the next section our trial functions are introduced. Section III provides the results of physical quantities by the VMC calculations. Energies and various correlation functions are compared with the exact calculations in Sec. III A. In Sec. III B, the correlation exponents are evaluated from the finite-size scaling to discuss the long-range behavior of correlation functions. The phase diagram of the 1D t-J model determined by our wave functions is shown in Sec. III C. Section VI is devoted to a summary and discussion of related problems.

II. TRIAL WAVE FUNCTION

The t-J model is defined by the Hamiltonian

$$H=-t\sum_{\langle ij\rangle\sigma}(\hat{c}_{i\sigma}^{\dagger}\hat{c}_{j\sigma}+\text{H.c.})+J\sum_{\langle ij\rangle}(\mathbf{S}_i\cdot\mathbf{S}_j-\tfrac{1}{4}n_in_j), \quad (1)$$

where $\hat{c}_{i\sigma}^{\dagger}=c_{i\sigma}^{\dagger}(1-n_{i,-\sigma})$, $c_{i\sigma}^{\dagger}$ being the creation operator for an electron with spin projection σ at lattice site i, and $n_i=\Sigma_\sigma n_{i\sigma}=\Sigma_\sigma c_{i\sigma}^{\dagger}c_{i\sigma}$. Thus $\hat{c}_{i\sigma}^{\dagger}$ creates an electron only on an empty site, avoiding double occupancy. The spin operator associated with site i is defined as $\mathbf{S}_i=\frac{1}{2}\Sigma_{\alpha,\beta}c_{i\alpha}^{\dagger}\boldsymbol{\sigma}_{\alpha,\beta}c_{i\beta}$, where $\boldsymbol{\sigma}=(\sigma_x,\sigma_y,\sigma_z)$ is a vector of Pauli matrices. The summations in Eq. (1) are taken over nearest-neighboring pairs. This model reduces to the $U=\infty$ Hubbard model in the limit $J/t\to 0$.

For highly correlated electron systems, Gutzwiller-Jastrow-type wave functions with a two-body correlation factor are fairly common.[14–19] The Gutzwiller wave function,[20] which is a prototype of the trial function of this type, is often used as a starting trial function for its simplicity. It is defined as

$$|\psi_G\rangle=P_d|\phi_F\rangle=\prod_i(1-n_{i\uparrow}n_{i\downarrow})|\phi_F\rangle, \quad (2)$$

where ϕ_F is a simple Fermi sea and P_d is the operator projecting out the double occupancy. This wave function is essentially a Fermi-liquid state, having a discontinuity in momentum distribution at $k=k_F$. Thus, the expected TLL behavior was not recovered.[17] Hellberg and Mele have introduced a variational state with a long-range correlation:[18]

$$|\psi_{\text{HM}}\rangle=\prod_{i\neq j}\prod_{\sigma\sigma'}[1-(1-|d_{ij}|^{\nu})n_{i\sigma}n_{j\sigma'}]|\psi_G\rangle, \quad (3)$$

$$d_{ij}=\sin[\pi r_{ij}/N_s], \quad (4)$$

where $r_{ij}=|r_i-r_j|$ is the distance between the ith and jth sites, and N_s the number of sites. When $\nu=0$, ψ_{HM} reduces to ψ_G. It has been shown that ψ_{HM} exhibits the characteristic behavior of a TLL.[18] However, the correlation exponent estimated with this wave function does not coincide with the exact value for small J/t.[19] This disagreement becomes apparent when the global features of various correlation functions are compared with the exact ones.[19]

An important feature of the TLL is the separation of spin and charge degrees of freedom in the low-energy excitations. In the limit of $J/t\to 0$, Ogata and Shiba have shown that the ground-state wave function obtained from the Bethe ansatz has a simple form due to the complete decoupling of charge and spin degrees of freedom.[10] It can be written as a product of a Slater determinant of spinless fermions describing the charge degrees of freedom and the spin wave function of the squeezed Heisenberg model in which all empty sites are omitted. The ground-state wave function in the limit of $J/t\to 0$ is expressed as

$$\psi_0(x_1,\ldots,x_{N_e})=X(x_1,\ldots,x_{N_e})Y(y_1,\ldots,y_M), \quad (5)$$

where

$$X(x_1,\ldots,x_{N_e})=\det[\exp(iq_ix_j)], \quad (6)$$

$\{x_j\}$ are the positions of N_e electrons, and $\{y_j\}$ are the coordinates of M up spins with vacant sites omitted. $X(x_1,\ldots,x_{N_e})$ is the wave function for noninteracting spinless fermions with momenta $\{q_i\}$, and $Y(y_1,\ldots,y_M)$ is the ground-state wave function of the $S=\frac{1}{2}$ antiferromagnetic Heisenberg model.

For finite values of J/t, the charge and spin degrees of freedom are no longer completely separated, and the charge-spin coupling occurs. Thus we introduce a Jastrow-type correlation factor in our trial wave function to mix the charge and spin degrees of freedom. We shall study the following variational state for the 1D t-J model:

$$|\psi_{\text{BA}}\rangle=F_J|XY\rangle, \quad (7)$$

where the amplitude of $|X\rangle=\Pi_i^{N_e}c_{q_i}^{\dagger}|0\rangle$ is given by Eq. (6), ensuring the absence of double occupancy. The long-range correlation factor of Jastrow type in Eq. (7) is defined as

$$F_J=\prod_{i\neq j}\prod_{\sigma\sigma'}\{1-[1-\eta(r_{ij};\sigma\sigma')]n_{i\sigma}n_{j\sigma'}\}, \quad (8)$$

and the form of function η is assumed to be

$$\eta(r_{ij};\sigma\sigma')=\begin{cases}|d_{ij}|^{\nu_1} & \text{if} \quad \sigma=\sigma',\\ |d_{ij}|^{\nu_2} & \text{if} \quad \sigma\neq\sigma',\end{cases} \quad (9)$$

where d_{ij} is given by Eq. (4). The Jastrow factor F_J modulates the Bethe-ansatz wave function by the distance between

all pairs of particles. A positive value of ν_1 (ν_2) induces a repulsive correlation between particles with the same spins (opposite spins), while negative values provide an attractive correlation. When $\nu_1=\nu_2$, F_J reduces to the correlation factor studied by Hellberg and Mele.

The wave function of the spin part in Eq. (7) is approximated as a trial function of Jastrow-Marshall-type,[23]

$$Y(y_1,\ldots,y_M)=(-1)^{L\{y_i\}}\prod_{i<j}|s_{ij}|^{\nu_s}, \tag{10}$$

where $s_{ij}=\sin[\pi(y_i-y_j)/N_e]$ for a system of N_e electrons and $L\{y_i\}$ is the number of up spins in one sublattice contained in the spin configuration $(y_1,\ldots,y_M)$. With this trial function $Y(y_1,\ldots,y_M)$, we have calculated the ground-state energies of the 1D antiferromagnetic Heisenberg model, $H_{\rm Heis}=J\Sigma_{\langle ij\rangle}\mathbf{S}_i\cdot\mathbf{S}_j$, with $N_e\leqslant 70$ by the VMC technique, and estimated the energy in the thermodynamic limit from finite-size scaling with a formula $E/N_e=E_\infty+C/N_e^2$. The minimum energy is realized for $\nu_s\approx 2$, and the resultant energy is $E_\infty=(-0.4421\pm 0.0001)J$, which is quite close to the exact value by the Bethe ansatz,[24] $E_{\rm BA}/N_e=-(\ln 2-\frac{1}{4})J=(-0.443\,147\ldots)J$. The difference is only 0.24%. Therefore, $Y(y_1,\ldots,y_M)$ reproduces well the true ground-state wave function of the 1D Heisenberg model.

As a result, we have three variational parameters in our trial state (7), i.e., ν_1, ν_2, and ν_s. In most regions of the phase diagram, this wave function $\psi_{\rm BA}$ successfully reproduces the exact ground state of the 1D t-J model as shown in Sec. III.

However, a Luther-Emery-liquid behavior, exhibiting a gap in the spin excitation spectrum and enhanced superconducting correlations, is found for $J>2t$ and at small densities.[6,7] The true ground state for this region lies out of the variational subspace spanned by $\psi_{\rm BA}$. To represent the spin-gap phase better, we introduce another trial state as follows:

$$|\psi_{\rm RVB}\rangle=F_J P_d\sum_{\{i_n j_n\}}\prod_{n}^{N_e/2} h^{r_{i_n j_n}-1}[i_n,j_n]|0\rangle, \tag{11}$$

where $[i,j]=(c^\dagger_{i\uparrow}c^\dagger_{j\downarrow}-c^\dagger_{i\downarrow}c^\dagger_{j\uparrow})$ is a singlet pair in a given configuration $\{i_n j_n\}$, and P_d projects out the double occupancy. In Eq. (11), $h^{r_{ij}-1}$ controls the weight for a singlet bond as a function of its length. The function η in the Jastrow factor is taken to be $\eta(r_{ij};\sigma\sigma')=|d_{ij}|^\lambda$; i.e., F_J is assumed to be spin independent. Two variational parameters λ and h are contained in the trial function $\psi_{\rm RVB}$. This is a natural generalization of the wave function of a gas of noninteracting bound singlet pairs proposed by Chen and Lee,[6] which corresponds to a Luther-Emery state with infinite correlation exponent. Correlating the singlet pairs with the Jastrow factor F_J, $\psi_{\rm RVB}$ can be expected to exhibit generalized Luther-Emery behavior. It is also a particular form of the resonating valence bond (RVB) state. In fact, $\psi_{\rm RVB}$ can be rewritten as

$$|\psi_{\rm RVB}\rangle=F_J P_d\left[\sum_k \frac{\cos k-h}{h^2-2h\cos k+1}c^\dagger_{k\uparrow}c^\dagger_{-k\downarrow}\right]^{N_e/2}|0\rangle, \tag{12}$$

which explicitly shows a singlet liquid picture of the RVB state.[2]

III. SIMULATION AND RESULTS

In this section, we present the results of the VMC calculations for various values of J/t and $n_e=N_e/N_s$ with N_e and N_s being the number of electrons and sites, respectively, and make comparisons with those of exact calculations and other trial functions. We consider the 1D t-J model with up to 300 sites under the periodic boundary condition with $N_e/2=$ odd.

The variational parameters in Eqs. (7) and (11) are optimized using a conjugate-gradient method combined with the fixed sampling in the VMC calculations. Technical details of the optimization procedure were described in Ref. 25, and some practical improvements are made to achieve the convergence rapid enough to handle multiparameter optimization: A quasi-Newton algorithm is employed instead of Powell's optimization algorithm in Ref. 25, and the gradient is evaluated by the numerical differentiation. Once the fully optimized wave function is obtained, we use it in evaluating the physical quantities with another VMC run in order to examine the properties of the 1D t-J model in detail. Calculated quantities are the total energy per site, the momentum distribution function

$$n(k)=\frac{1}{2N_s}\sum_{ij\sigma} e^{ik(r_i-r_j)}\langle c^\dagger_{i\sigma}c_{j\sigma}\rangle, \tag{13}$$

and the equal-time correlation functions, where $\langle\cdots\rangle$ indicates the expectation value for a given trial function. The spin and charge correlation functions in Fourier-transformed form are defined as

$$S(k)=\frac{4}{N_s}\sum_{ij} e^{ik(r_i-r_j)}\langle S^z_i S^z_j\rangle, \tag{14}$$

$$C(k)=\frac{1}{N_s}\sum_{ij} e^{ik(r_i-r_j)}[\langle n_i n_j\rangle-\langle n_i\rangle\langle n_j\rangle], \tag{15}$$

respectively. The singlet pairing correlation function is defined as

$$P(k)=\frac{1}{N_s}\sum_{ij} e^{ik(r_i-r_j)}\langle\Delta^\dagger_i\Delta_j\rangle, \tag{16}$$

where Δ_i is the annihilation operator of a nearest-neighboring electron singlet pair,

$$\Delta_i=\frac{1}{\sqrt{2}}(c_{i\uparrow}c_{i+1\downarrow}-c_{i\downarrow}c_{i+1\uparrow}). \tag{17}$$

We collect typically 30 000 samples to take averages of the energy for the optimization of variational parameters, and 100 000–200 000 samples for the evaluations of the expectation values of observables.

A. Quarter-filled case

First we compare the properties of $\psi_{\rm BA}$ with those of $\psi_{\rm HM}$ for the quarter-filled case: $n_e=\frac{1}{2}$. At this electron den-

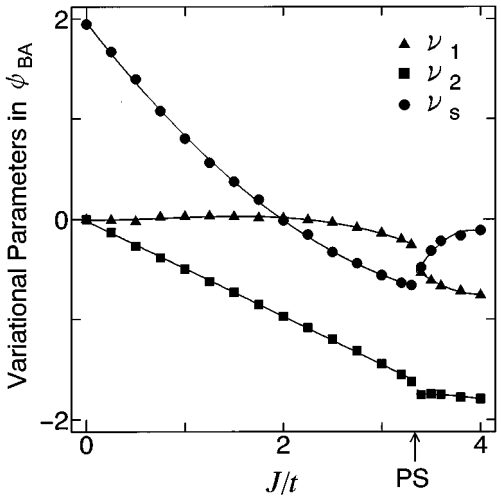

FIG. 1. Optimization result of variational parameters in ψ_{BA} is shown for $n_e=\frac{1}{2}$ and $N_s=100$. Triangles, squares, and circles represent ν_1, ν_2, and ν_s, respectively. The solid lines are the least-squares fits of the data. The transition to a phase-separated state is shown by an arrow at $J/t\approx 3.3$.

sity, the spin-gap state is absent. In addition, when $J/t\to 0$, the exact results of correlation functions have been obtained[10,17,26] for fairly large N_s, with which we can compare the VMC results.

The result of the optimization of variational parameters in ψ_{BA} is shown in Fig. 1 for $n_e=1/2$ as a typical case. The data in the region $J/t\leqslant 3.3$ are fitted to polynomials of degree m, where $m=2$ for ν_2 and ν_s, and $m=3$ for ν_1, respectively. For $J/t\to 0$, the minimum energy is realized for $\nu_1=\nu_2=0$ and $\nu_s\approx 2$. In the case of finite J/t, the optimal variational parameters show the coupling of charge and spin degrees of freedom as expected, i.e., $\nu_1\neq 0$ and/or $\nu_2\neq 0$. ν_2 and ν_s decrease with J/t while the dependence of ν_1 on J/t is weak for $J/t\leqslant 2$. Near $J/t=2$, ν_s intersects the zero line, and ν_2 becomes -1. For larger J/t, the attractive correlation between electrons with opposite spins is prominent. For $J/t>3.3$, the variational state separates into the electron-rich and -poor phases. The variational parameters abruptly change their behavior at the phase separation boundary as shown in Fig. 1. The data in the phase separated region are fitted to other polynomials.

For other values of n_e, the optimal values of variational parameters show similar behaviors except for curvatures. Notice that the trial state with optimal variational parameters is single although the Jastrow factor F_J is spin dependent; the VMC evaluation of the physical quantities shows that the total spin is zero, and the spin correlation function is isotropic $[S^{xx}(k)=S^{yy}(k)=S^{zz}(k)]$, as far as the optimized ψ_{BA} is employed.[27]

Next we discuss the variational energies. It has been shown that the ground-state energy converges smoothly to the thermodynamic limit.[17,19] Following Yokoyama and Ogata,[17,19] we estimate the variational energy per site in the limit $N_s\to\infty$ from the finite-size scaling. We calculate the variational energies of 12-, 20-, 36-, 60-, and 100- site systems for $n_e=0.5$ using the optimized ψ_{BA} and ψ_{HM}, and then fit the results to the formula

$$E/N_s=E_\infty+C_1/N_s^2+C_2/N_s^4+C_3/N_s^6. \tag{18}$$

The fitted values of $E_\infty(\psi_{\mathrm{BA}})$ and $E_\infty(\psi_{\mathrm{HM}})$ are listed in Table I for several values of J/t. They are compared to the exact results obtained from the Bethe ansatz for $J/t=0$ (Ref. 28) and 2,[29] and the extrapolated values of the exact diagonalization of small clusters for $J/t=1$ and 3. The latter is evaluated from fitting the energies of 4-, 8-, 12-, and 16- site clusters to Eq. (18).[19]

Using ψ_{BA}, the ground-state energy per site in the limit $N_s\to\infty$ is obtained to be $E_\infty=-2t/\pi$ for $J/t\to 0$, equivalent to the exact energy. The reason for the coincidence is that the energy is determined only by the charge degree of freedom in the limit $J/t\to 0$, whose treatment is rigorous in ψ_{BA}. In fact, the variance $\langle[H-E(\psi_{\mathrm{BA}})]^2\rangle$ in VMC sweeps vanishes at any n_e. For all the range of J/t, $E_\infty(\psi_{\mathrm{BA}})$ is quite close to the exact energy, as shown in Table I. Especially in the small J/t region, the advantage of ψ_{BA} over ψ_{HM} is obvious. The difference in energy between ψ_{HM} and the exact one is largest for $J/t=0$, while the error of ψ_{BA} gradually increases with J/t except for $J/t=2$.

For $J/t=2$, both $E_\infty(\psi_{\mathrm{BA}})$ and $E_\infty(\psi_{\mathrm{HM}})$ are extremely close to the exact energy obtained by the Bethe ansatz. In this connection, Yokoyama and Ogata have shown that the Gutzwiller function ψ_G is a good trial function for $J/t=2$ and all range of n_e.[17] In fact, an analytical calculation of the energy using the Gutzwiller wave function shows $E_\infty(\psi_G)=-0.903\,092\ldots$,[30,17] which is close to the exact one. Moreover, Kuramoto and Yokoyama[31] have found that ψ_G is the exact ground state of the t-J model with long-range interactions and hoppings satisfying $J_{ij}=2t_{ij}\propto r_{ij}^{-2}$ In the supersymmetric case, the ground state behaves as almost a free-electron state[19] except for the exclusion of double occupancy because of the cancellation of hopping and interacting processes, both of which have the same weight $t=J/2$.

TABLE I. Ground-state energies of the 1D t-J model in the limit $N_s\to\infty$ for the quarter-filled case ($n_e=\frac{1}{2}$). The VMC results are obtained from the finite-size scaling, Eq. (18), with $N_s=$ 12, 20, 36, 60, and 100. Exact results obtained from the Bethe ansatz for $J=0$ (Ref. 28) and 2 (Ref. 29) and extrapolated values of the exact diagonalization of small clusters (Ref. 19) for $J=1$ and 3 are listed as a comparison. The unit of the energy is t.

J	Exact	VMC $E_\infty(\psi_{\mathrm{HM}})$		(Error %)	VMC $E_\infty(\psi_{\mathrm{BA}})$		(Error %)
0	−0.636620	−0.6119	± 0.0003	(4)	−0.636620	± 0	(0)
1	−0.755359	−0.7493	± 0.0001	(0.8)	−0.75488	± 0.00005	(0.06)
2	−0.903649	−0.90315	± 0.00005	(0.06)	−0.90318	± 0.00006	(0.05)
3	−1.081713	−1.0774	± 0.0001	(0.4)	−1.0806	± 0.0001	(0.1)

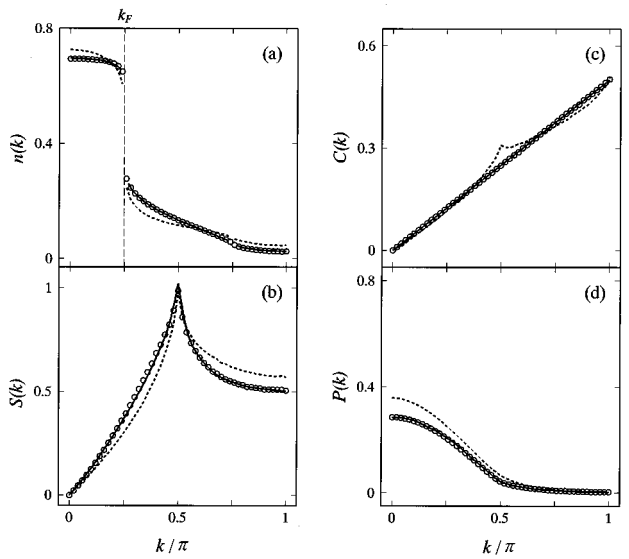

FIG. 2. (a) The momentum distribution function $n(k)$, (b) the spin correlation function $S(k)$, (c) the charge correlation function $C(k)$, and (d) the singlet pairing correlation function $P(k)$ for $n_e=\frac{1}{2}$ and $J/t=0$. Open circles and dashed lines denote the VMC results of $\psi_{\rm BA}$ and $\psi_{\rm HM}$, respectively, for $N_s=100$. The exact results (Refs. 10,17, and 26) for $N_s=52$ are also shown with solid lines.

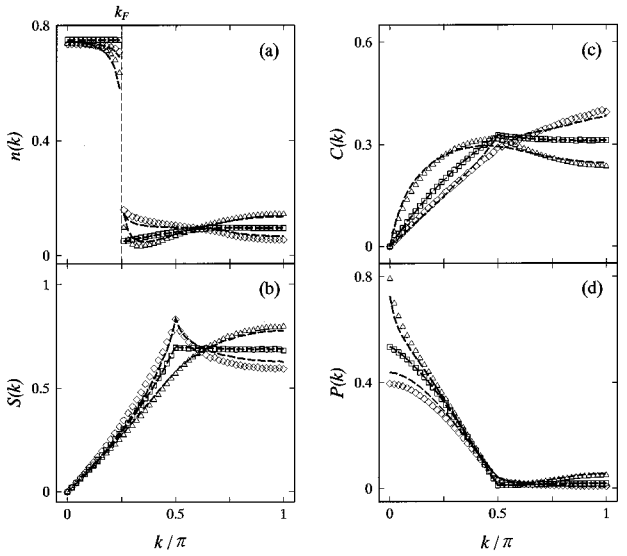

FIG. 3. (a) The momentum distribution function $n(k)$, (b) the spin correlation function $S(k)$, (c) the charge correlation function $C(k)$, and (d) the singlet pairing correlation function $P(k)$ for $n_e=\frac{1}{2}$ and $N_s=100$. The data are evaluated by the VMC calculations with $\psi_{\rm BA}$ for $J/t=1$ (open diamonds), 2 (open squares), and 3 (open triangles). The dashed lines denote the corresponding results of $\psi_{\rm HM}$.

Therefore, it is natural to expect that variational energies converge to the same value if a trial function can recover the ''free-electron'' nature for $J/t=2$. The above three variational wave functions have this property correctly although the long-range behavior of correlation functions is different.

In Fig. 2, (a) the momentum distribution function $n(k)$, (b) the spin correlation function $S(k)$, (c) the charge correlation function $C(k)$, and (d) the singlet pairing correlation function $P(k)$ are shown for $J/t=0$, where open circles denote the VMC results of $\psi_{\rm BA}$, and the dashed lines represent those of $\psi_{\rm HM}$. We evaluate the data for the lattice with 100 sites at quarter filling. The exact results obtained from the Bethe-ansatz solution for $N_s=52$ are also shown in Fig. 2 with solid lines.[10,17,26] In the TLL, the momentum distribution function exhibits power-law singularities at k_F and $3k_F$ although the latter is very weak. Qualitatively, both of $\psi_{\rm BA}$ and $\psi_{\rm HM}$ reproduce the anomalous power-law behavior inherent in a TLL as shown in Fig. 2(a). However, $n(k)$ by $\psi_{\rm HM}$ departs appreciably from that by the Bethe ansatz while $n(k)$ by $\psi_{\rm BA}$ almost coincides with the exact one. For the correlation functions, there are also the apparent differences between $\psi_{\rm HM}$ and the exact result while $\psi_{\rm BA}$ is quite close to the exact one, as shown in Figs. 2(b)–2(d). In particular, $C(k)$ calculated with $\psi_{\rm HM}$ shows different behavior: It has a small cusp at $2k_F$. On the other hand, both $\psi_{\rm BA}$ and the exact result exhibit linear k dependence in $C(k)$, reflecting the free spinless fermions nature. Thus $\psi_{\rm BA}$ recovers the global features of correlation functions correctly in contrast to $\psi_{\rm HM}$.

In Fig. 3, we show the VMC results of the momentum distribution function and the correlation functions for finite J/t and $n_e=\frac{1}{2}$. We have plotted the results of $\psi_{\rm BA}$ (open symbols) and $\psi_{\rm HM}$ (dashed lines) for comparison. At $J/t=1$ (open diamonds), the difference between $\psi_{\rm BA}$ and $\psi_{\rm HM}$ is observed, but it is not so large as in the case of $J/t=0$ except for the peak of $C(2k_F)$. For $J/t=2$ (open squares), the two variational functions give almost the same results, in accordance with the agreement of energies. At $J/t=3$ (open triangles), it is remarkable that $P(k)$ at $k=0$ is strongly enhanced due to the increased effective attraction between neighboring electrons with opposite spins as shown in Fig. 3(d). One can also see the enhancement of $P(k)$ near $k=\pi$ as J/t increases. The singularity of $P(2k_F)$ becomes sharp when $J/t=2$.

The correlation functions by $\psi_{\rm BA}$ shown in Fig. 3 agree well with the result of the quantum Monte Carlo calculation[32] or of the exact diagonalization in smaller lattices.[17,19,26]

B. Correlation exponent

Let us now examine the correlation exponents to discuss the long-range behavior of correlation functions. In the TLL regime, both the charge and spin excitations are gapless and the correlation functions show power-law decay. Following the TLL theory, the leading singularities of the distribution function and correlation functions can be written as[4,8]

$$n(k)\sim|k-k_F|^{\alpha}\,\mathrm{sgn}(k-k_F)\quad\text{for } k\sim k_F, \tag{19}$$

$$S(k)\sim|k-2k_F|^{\eta-1}\quad\text{for } k\sim 2k_F, \tag{20}$$

$$C(k)\sim|k-2k_F|^{\eta-1}\quad\text{for } k\sim 2k_F, \tag{21}$$

$$P(k)\sim|k|^{\mu-1}\quad\text{for } k\sim 0. \tag{22}$$

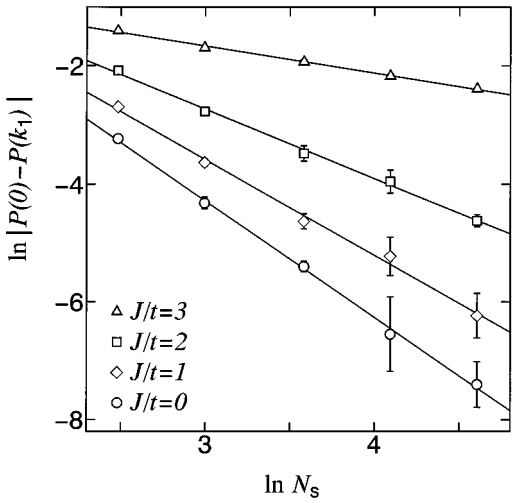

FIG. 4. The VMC results of $\ln|P(0)-P(k_1)|$ at $n_e=1/2$ are plotted for $J/t=0$ (circles), 1 (diamonds), 2 (squares), and 3 (triangles) as a function of $\ln N_s$, where $k_1=2\pi/N_s$. The data are evaluated with ψ_{BA} for $N_s=$ 12, 20, 36, 60, and 100. The solid lines are the least-squares fits of the plots.

Logarithmic corrections have been omitted in these formulas. As far as the interaction is isotropic in spin space, the critical exponents are described by a dimensionless TLL parameter K_ρ as follows:[4,8]

$$\alpha=\min[1,(K_\rho-1)^2/(4K_\rho)], \tag{23}$$

$$\eta=K_\rho+1, \tag{24}$$

$$\mu=1/K_\rho+1. \tag{25}$$

The correlation exponent K_ρ can now be rather easily calculated from our VMC result of $P(k)$ than $n(k)$, $C(k)$, or $S(k)$ since the singularities of these quantities become much weaker than that of $P(k)$ in some cases. Following Assaad and Würtz,[32] we use the following procedure to obtain the exponent of $P(k)$. Let us assume a behavior

$$\ln|P(0)-P(k_1)|=-(\mu-1)\ln N_s+a, \tag{26}$$

where $k_1=2\pi/N_s$, and μ and a are the fitting parameters. Fitting the data for various lattice sizes to Eq. (26), the exponent of $P(k)$ can be evaluated by finite-size scaling. Once μ is obtained, K_ρ is given by Eq. (25).

As an example, we plot the fitting result of $P(k)$ for $n_e=\frac{1}{2}$ in Fig. 4. We have calculated $P(k)$ of 12-, 20-, 36-, 60-, and 100-site systems for $n_e=\frac{1}{2}$ using the optimized ψ_{BA}, and then fit the results to Eq. (26). The linearity of these plots is good. The correlation exponent K_ρ obtained from the slope of these plots and Eq. (25) is tabulated in Table II. For ψ_{HM}, one can rather analyze the exponent directly. The relation between the variational parameter in ψ_{HM} and K_ρ has been derived analytically from the generalized conformal field theoretical argument to be[33]

$$K_\rho=\frac{1}{2\nu+1}. \tag{27}$$

TABLE II. The correlation exponent K_ρ for $n_e=\frac{1}{2}$. Results for ψ_{BA} are evaluated from fitting $P(k)$ to Eq. (26) for lattice sizes ranging from $N_s=12$ to 100. With ψ_{HM}, K_ρ is directly obtained from Eq. (27). The last column is evaluated from the optimized variational parameters in ψ_{BA}.

J/t	Expected value	$K_\rho(\psi_{\mathrm{HM}})$	$K_\rho(\psi_{\mathrm{BA}})$	$(\nu_1+\nu_2+2)^{-1}$
0	0.50 [a]	0.40	0.51 ± 0.03	0.50
1	0.62 [b]	0.57	0.62 ± 0.05	0.65
2	0.85 [c]	0.95	0.85 ± 0.07	0.95
3	2.2 [b]	3.2	2.2 ± 0.2	2.4

[a]References 34 and 35.
[b]Reference 5.
[c]Reference 36.

Therefore, the optimal value of ν can be used to determine K_ρ for ψ_{HM}. The results for ψ_{HM} in Table II are obtained from this equation. The expected values of the exponents are also shown in Table II: For $J/t=0$ and 2, K_ρ has been exactly determined from the bosonization theory[34] or the conformal field theory,[35,36] with $K_\rho=0.5$ and 0.85, respectively, and the exact diagonalization on a 16-site ring has shown[5] that $K_\rho\approx0.62$ and 2.2 for $J/t=1$ and 3, respectively.

The results of ψ_{HM} and ψ_{BA} are consistent with the expected values; at $J/t=3$, K_ρ becomes larger than 1 and thus the superconducting correlations correspondingly dominate the long-range behavior while for smaller value of J/t, $K_\rho<1$. However, the quantitative coincidence is not so good for ψ_{HM}, while the exponents evaluated from ψ_{BA} are surprisingly close to the expected values. Therefore, one could conclude that our variational wave function ψ_{BA} can quantitatively reproduce not only the amplitude of correlation functions, but also the correlation exponent. The last column in Table II shows the value of $(\nu_1+\nu_2+2)^{-1}$ evaluated from the optimized variational parameters in ψ_{BA}. It seems that K_ρ agrees with $(\nu_1+\nu_2+2)^{-1}$. This point will be discussed in the next subsection.

C. Phase diagram

The phase diagram of the 1D t-J model obtained by ψ_{BA} and ψ_{RVB} is shown in Fig. 5 with contour lines for several values of K_ρ. As seen in Fig. 5, there are four distinct phases. For small J/t, the ground state is a repulsive TLL with $K_\rho<1$. In this region, spin correlations dominate the long-range behavior. Increasing J/t, these correlations are suppressed, and the ground state changes to an attractive TLL with $K_\rho>1$. It has dominant singlet pairing correlations. For larger J/t, the variational state is phase separated into the electron-rich phase with antiferromagnetic order and the empty phase. In this region, the longest-wavelength charge correlation $C(k_1=2\pi/N_s)$ diverges when the system size N_s is increased. This behavior is in contrast with the TLL, where $C(k_1)$ remains finite. The phase separation boundary in Fig. 5 is determined by the behavior of $C(k_1)$. These three phases are described by ψ_{BA}. The spin-gap state lies between the TLL and phase-separated regions at small densities, where ψ_{RVB} is more stable than ψ_{BA}. The optimal values of variational parameters in ψ_{RVB} fit to the formulas

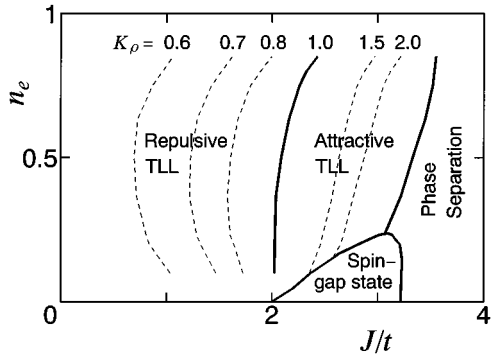

FIG. 5. The phase diagram of the 1D t-J model as determined by ψ_{BA} and ψ_{RVB}. In the spin-gap phase, ψ_{RVB} is more stable than ψ_{BA} while other phases are described by ψ_{BA}. The curves represent the contours of constant correlation exponent K_ρ evaluated from Eq. (29).

as $h=1.037-0.151(J/t)$ and $\lambda=0.781-0.173(J/t)$ for $n_e=0.2$ and $2.8\leqslant J/t\leqslant 3.2$, for example.

The phase diagram determined by the present method is consistent with the result of the exact diagonalization on a 16-site ring.[5] It is correctly recovered that $K_\rho=1/2$ at any electron density in the limit $J/t\rightarrow 0$.[34,35] When we compare the spin-gap region with the result of the wave function of noninteracting singlet pairs by Chen and Lee,[6] the correlation effect of the Jastrow factor introduced in ψ_{RVB} seems to play no essential role since these two trial functions give almost the same result; the correlation effect only slightly pushes the spin-gap region to larger values of n_e. This is because the balance of energy hardly changes; i.e., the magnitude of correlation energy induced by the Jastrow factor in ψ_{RVB} is less than 2%, which is comparable to the energy lowering of ψ_{BA} compared to ψ_{HM}. However, there is a significant difference in the long-range behavior of correlation functions. The wave function by Chen and Lee gives $K_\rho=\infty$ while K_ρ is finite for our ψ_{RVB} as seen below.

Figure 6 shows the distribution function and correlation functions for 150 sites and 30 electrons. The selected values of J/t are 0, 2.5, and 3 as typical cases of the repulsive TLL, attractive TLL, and spin-gap state, respectively. Triangles and squares in Fig. 6 are evaluated with ψ_{BA} while circles with ψ_{RVB}. The spin correlation functions for $J/t=0$ and 2.5 exhibit the linear behavior at small k characteristic of the TLL as shown in Fig. 6(b). On the other hand, $S(k)$ for $J/t=3$ is quadratic at small k and analytic for all wave vectors. Unlike TLL's, a Luther-Emery liquid exhibits exponential decay of the spin correlation function in real space, while both charge and singlet pairing correlations decay algebraically.[8] The short-range behavior of $S(k)$ for $J/t=3$ shows that the spin-gap state is characterized as a Luther-Emery liquid. The charge correlation function for $J/t=3$ exhibits a cusp at $k=2k_F$, indicating the formation of bound singlet pairs. As J/t decreases, this cusp is suppressed. More definitive characters of the three phases can be seen in the singlet pairing correlation functions plotted in Fig. 6(d). $P(k)$ is fully suppressed when $J/t=0$. As J/t increases, $P(k=0)$ becomes much larger, indicating the growth of long-range order. The cusp at $k=0$ is greatly enhanced for $J/t=3$.

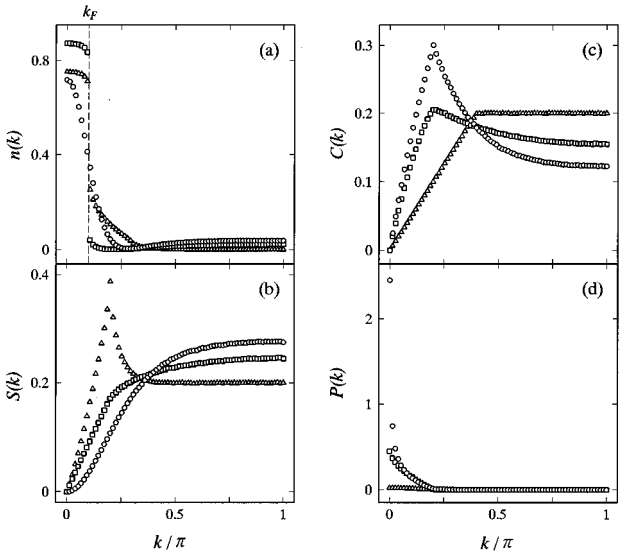

FIG. 6. (a) The momentum distribution function $n(k)$, (b) the spin correlation function $S(k)$, (c) the charge correlation function $C(k)$, and (d) the singlet pairing correlation function $P(k)$ for $n_e=0.2$ and $N_s=150$. Selected values of J/t are 0 (triangles), 2.5 (squares), and 3 (circles) as typical cases of the repulsive TLL, attractive TLL, and spin-gap state, respectively.

Finally, we plot the exponents of the singlet pairing correlation function for $n_e=0.2$ as a function of J/t in Fig. 7, where $\mu-1$ is evaluated from fitting $P(k)$ to Eq. (26) for lattice sizes ranging from $N_s=30$ to 150. In the region $2.8\leqslant J/t\leqslant 3.2$, the variational energy of ψ_{RVB} is lower than that of ψ_{BA}. Correspondingly, the squares and circles in Fig. 7 are evaluated with ψ_{BA} and ψ_{RVB}, respectively. In addition, $\nu_1+\nu_2+2$ for ψ_{BA} and $2\lambda-1$ for ψ_{RVB} are shown in Fig. 7 with solid lines, where ν_1, ν_2, and λ are optimized variational parameters. It seems that the fits of $\nu_1+\nu_2+2$

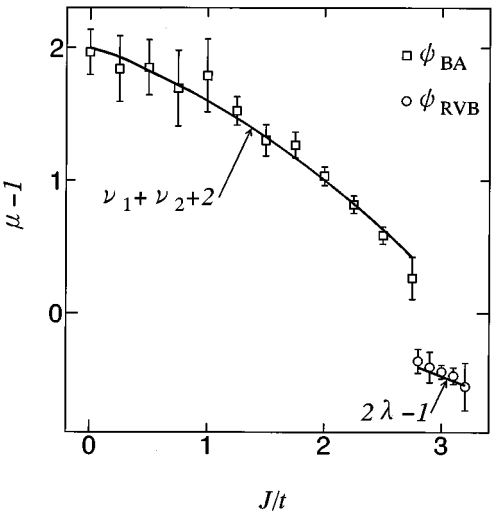

FIG. 7. Exponents of the singlet pairing correlation function for $n_e=0.2$ as a function of J/t. Squares are evaluated with ψ_{BA}, while circles with ψ_{RVB}, fitting $P(k)$ to Eq. (26) for lattice sizes ranging from $N_s=30$ to 150. Solid lines represent the value of $\nu_1+\nu_2+2$ for ψ_{BA} and $2\lambda-1$ for ψ_{RVB}, where ν_1, ν_2, and λ are the optimized variational parameters.

TABLE III. The correlation exponent K_ρ for $n_e=0.2$, obtained by fitting $P(k)$ to Eq. (26) for lattice sizes ranging from $N_s=30$ to 150. The last column is evaluated from the optimized variational parameters in the trial wave functions.

J/t	Type of ψ	K_ρ	$(\nu_1+\nu_2+2)^{-1}$ or $(2\lambda)^{-1}$
0.0	BA	0.51 ± 0.05	0.50
1.0	BA	0.57 ± 0.07	0.63
2.0	BA	0.97 ± 0.06	0.98
2.5	BA	1.7 ± 0.2	1.6
2.8	RVB	1.6 ± 0.2	1.7
3.0	RVB	1.8 ± 0.2	1.9
3.2	RVB	2.3 ± 0.4	2.2

and $2\lambda-1$ to the exponents of $P(k)$ are good. The exponents of the correlation functions in the Luther-Emery liquid that decay with power laws can be also described by a single parameter K_ρ like a TLL,[8] and it holds that

$$\mu=\frac{1}{K_\rho}. \tag{28}$$

Using Eqs. (25) and (28), one can conclude from Fig. 7 that K_ρ relates to the variational parameters in $\psi_{\rm BA}$ and $\psi_{\rm RVB}$ as

$$K_\rho=\frac{1}{\nu_1+\nu_2+2} \quad \text{for } \psi_{\rm BA} \tag{29}$$

and

$$K_\rho=\frac{1}{2\lambda} \quad \text{for } \psi_{\rm RVB}, \tag{30}$$

respectively. The critical exponent K_ρ evaluated from $P(k)$ for $n_e=0.2$ is tabulated in Table III together with the predicted values by Eqs. (29) and (30), and they agree very well. For other values of n_e, K_ρ also agrees with $(\nu_1+\nu_2+2)^{-1}$ or $(2\lambda)^{-1}$. The example for $n_e=0.5$ is shown in Table II. K_ρ shown in Fig. 5 is evaluated from Eq. (29).

The relations (29) and (30) are confirmed by the following facts. (i) In the limit $n_e\to 1$, we have $\nu_1=\nu_2=0$ and $\nu_s\approx 2$, i.e., $\psi_{\rm BA}=Y$, for the Heisenberg chain since X becomes only a constant. This is in accordance with $K_\rho\to 1/2$ as $n_e\to 1$.[5] (ii) It is correctly recovered that $K_\rho\to 1/2$ at any electron density in the limit $J/t\to 0$,[34,35] where we have $\nu_1=\nu_2=0$. (iii) The magnitude of the discontinuous jump in $\mu-1$ at $J/t\sim 2.8$ is $(\nu_1+\nu_2+2)-(2\lambda-1)\approx 1$ as seen in Fig. 7. This is consistent with the crossover from the TLL to the Luther-Emery-liquid behavior described by Eqs. (29) and (30). (iv) $\nu_1+\nu_2+2\approx 0$ on the phase separation boundary in Fig. 5, which leads to $K_\rho=\infty$. This corresponds to the divergence of $C(k_1)$.

IV. SUMMARY AND DISCUSSION

In this paper, we have carried out the VMC calculation for the 1D t-J model. As a trial state, we have proposed a variational wave function based on the Bethe-ansatz solution. In this wave function, the separation of charge and spin degrees of freedom is realized explicitly, and the long-range correlation factor of Jastrow type is included. With this wave function, it has been shown that remarkable improvement is achieved especially in the small J/t region: The variational energy, momentum distribution function, and various correlation functions exhibit an excellent coincidence with exact ones. The evaluation of correlation exponents with finite-size scaling has shown that this variational wave function can correctly reproduce not only the global features of correlation functions but also the long-range behavior with anomalous power-law decay, which is characteristic of a TLL.

In addition, a variational wave function of singlet pairs correlated with a Jastrow factor has been introduced to describe the spin-gap phase. This wave function correctly exhibits enhanced superconducting correlations and exponential decay of the spin correlation function, as expected for the generalized Luther-Emery state.

Comparing the energies of the trial function based on the Bethe-ansatz solution and the generalized Luther-Emery state, the whole phase diagram has been determined. The VMC results show that our wave functions provide a more precise description of the ground-state properties for the 1D t-J model in the whole phase diagram. Evaluating the correlation exponents by a finite-size scaling analysis, the relations between the exponent K_ρ and the variational parameters in the trial functions have been established.

Let us now compare our trial wave functions with others. For strongly correlated electron systems, the Gutzwiller-Jastrow-type trial state has been extensively studied, but the conventional Jastrow factor does not recover the expected TLL behavior if only short-range correlations are included.[17,19] A trial wave function of this type is essentially a Fermi-liquid state. The wave function introduced by Hellberg and Mele successfully exhibits the power-law singularity of the TLL.[18] The long-range nature of the Jastrow factor is essential for the non-Fermi-liquid behavior. However, the correlation exponent does not coincide with the exact value. This disagreement becomes apparent when we compare the global features of various correlation functions. The difference between $\psi_{\rm HM}$ and the exact result is largest for $J/t=0$. These are in sharp contrast to $\psi_{\rm BA}$, with which we can quantitatively reproduce both the amplitude and the exponent of correlation functions. This is because $\psi_{\rm BA}$ has the separation of charge and spin degrees of freedom correctly. The effect of the spin-charge separation becomes clear especially in the small J/t region. In fact, when we compare the phase diagram determined by the present method with that of $\psi_{\rm HM}$,[19] the behavior of K_ρ is much improved in the repulsive TLL region, while it agrees with the result of $\psi_{\rm HM}$ in the attractive TLL phase.

Finally we mention some remaining issues. The spin wave function $Y(y_1,\ldots,y_M)$ in Eq. (7) has been approximated as a trial function of Jastrow-Marshall type for its simplicity. It is known, however, a liquid state is realized in the 1D antiferromagnetic Heisenberg model. When a RVB-type trial state is used as the spin part in Eq. (7) instead of Jastrow-Marshall type, further improvement may be expected. Actually, Ogata[37] has examined a trial function composed of a spin trial state of RVB type and spinless fermions for $J/t=0$. It is interesting to correlate this trial function with a Jastrow factor, applying to all ranges of J/t.

An application of the present method with some modifi-

cations to magnetic properties such as spin susceptibility and magnetization curve is also interesting in order to elucidate the metal-insulator transition in the 1D t-J model. In fact, it was shown that Jastrow wave functions reproduce charge and spin susceptibilities and the magnetization curve correctly, in contrast with the Gutzwiller approximation.[19]

An important question is whether the properties of strongly correlated electrons realized in 1D system can be extended to higher dimensions because of their close connection to high-T_c superconductors.[12] In a 2D system, it is not established even for the metallic regime whether the ground state is a Fermi liquid or TLL. In these contexts, an extension of the present method to 2D systems together with a reexamination of the appropriate Hamiltonian is under consideration.

Quite recently, we have found that part of our result for the variational wave function of correlated singlet pairs has been obtained independently by Chen and Lee.[38]

ACKNOWLEDGMENTS

The authors are grateful to H. Yokoyama for useful comments. They wish to thank the Computer Center of the University of Tokyo for our utilization of the computer system for the numerical computation.

[1] J.G. Bednorz and K.A. Müller, Z. Phys. B **64**, 189 (1986).
[2] P.W. Anderson, Science **235**, 1196 (1987).
[3] F.C. Zhang and T.M. Rice, Phys. Rev. B **37**, 3759 (1988).
[4] For a review, see H. Shiba and M. Ogata, Prog. Theor. Phys. Suppl. **108**, 265 (1992).
[5] M. Ogata, M.U. Luchini, S. Sorella, and F.F. Assaad, Phys. Rev. Lett. **66**, 2388 (1991).
[6] Y.C. Chen and T.K. Lee, Phys. Rev. B **47**, 11 548 (1993).
[7] C.S. Hellberg and E.J. Mele, Phys. Rev. B **48**, 646 (1993).
[8] J. Sólyom, Adv. Phys. **28**, 201 (1979); V.J. Emery, in *Highly Conducting One-Dimensional Solids*, edited by J.T. Devreese, R.P. Evrard, and V.E. van Doren (Plenum, New York, 1979), p. 247.
[9] F.D.M. Haldane, Phys. Rev. Lett. **45**, 1358 (1980); J. Phys. C **14**, 2585 (1981).
[10] M. Ogata and H. Shiba, Phys. Rev. B **41**, 2326 (1990).
[11] For a review, see E. Dagotto, Rev. Mod. Phys. **66**, 763 (1994) and references therein.
[12] W.O. Putikka, R.L. Glenister, R.R.P. Singh, and H. Tsunetsugu, Phys. Rev. Lett. **73**, 170 (1994); Y.C. Chen and T.K. Lee, Z. Phys. B **95**, 5 (1994).
[13] For a review, see H. Yokoyama, Y. Kuramoto, and M. Ogata, in *Computational Physics as a New Frontier in Condensed Matter Research*, edited by H. Takayama *et al.* (The Physical Society of Japan, Tokyo, 1995), p. 160.
[14] C. Gros, R. Joynt, and T.M. Rice, Phys. Rev. B **36**, 381 (1987); H. Yokoyama and H. Shiba, J. Phys. Soc. Jpn. **56**, 1490 (1987).
[15] C. Gros, Ann. Phys. (N.Y.) **189**, 53 (1989).
[16] H. Yokoyama and H. Shiba, J. Phys. Soc. Jpn. **59**, 3669 (1990).
[17] H. Yokoyama and M. Ogata, Phys. Rev. Lett. **67**, 3610 (1991).
[18] C.S. Hellberg and E.J. Mele, Phys. Rev. B **44**, 1360 (1991); Int. J. Mod. Phys. B **5**, 1791 (1991); Phys. Rev. Lett. **67**, 2080 (1991).
[19] H. Yokoyama and M. Ogata, Phys. Rev. B **53**, 5758 (1996).
[20] M.C. Gutzwiller, Phys. Rev. Lett. **10**, 159 (1965).
[21] R. Valentí and C. Gros, Phys. Rev. Lett. **68**, 2402 (1992); C. Gros and R. Valentí, Mod. Phys. Lett. B **7**, 119 (1993); Phys. Rev. B **50**, 11 313 (1994).
[22] A. Luther and V. J. Emery, Phys. Rev. Lett. **33**, 589 (1974).
[23] W. Marshall, Proc. R. Soc. London, Ser. A **232**, 48 (1955); R. Jastrow, Phys. Rev. **98**, 1479 (1955). See also, E. Manousakis, Rev. Mod. Phys. **63**, 1 (1991).
[24] H.A. Bethe, Z. Phys. **71**, 205 (1931).
[25] K. Kobayashi and K. Iguchi, Phys. Rev. B **47**, 1775 (1993).
[26] T. Pruschke and H. Shiba, Phys. Rev. B **46**, 356 (1992).
[27] As discussed in Ref. 19, a wave function of Jastrow type generally becomes nonsinglet if the Jastrow factor composed of only diagonal elements is spin dependent. Elucidating the relation between ψ_{BA} and a Jastrow-type wave function with off-diagonal elements is left for future study.
[28] H. Shiba, Phys. Rev. B **6**, 930 (1972).
[29] P.-A. Bares and G. Blatter, Phys. Rev. Lett. **64**, 2567 (1990); P.-A. Bares, G. Blatter, and M. Ogata, Phys. Rev. B **44**, 130 (1991).
[30] W. Metzner and D. Vollhardt, Phys. Rev. B **37**, 7382 (1988); F. Gebhard and D. Vollhardt, *ibid.* **38**, 6911 (1988).
[31] Y. Kuramoto and H. Yokoyama, Phys. Rev. Lett. **67**, 1338 (1991).
[32] F.F. Assaad and D. Würtz, Phys. Rev. B **44**, 2681 (1991).
[33] N. Kawakami and P. Horsch, Phys. Rev. Lett. **68**, 3110 (1992); C.S. Hellberg and E.J. Mele, *ibid.* **68**, 3111 (1992).
[34] H.J. Schulz, Phys. Rev. Lett. **64**, 2831 (1990).
[35] N. Kawakami and S.-K. Yang, Phys. Lett. A **148**, 359 (1990); H. Frahm and V.E. Korepin, Phys. Rev. B **42**, 10 553 (1990).
[36] N. Kawakami and S.-K. Yang, Phys. Rev. Lett. **65**, 2309 (1990).
[37] M. Ogata, in *Correlation Effects in Low-Dimensional Electron Systems*, edited by A. Okiji and N. Kawakami (Springer-Verlag, Berlin, 1994), pp. 121–127.
[38] Y.C. Chen and T.K. Lee, Phys. Rev. B **54**, 9062 (1996).